polymers

MDPI

Article

Effect of Fiber Loading on Thermal Properties of Cellulosic Washingtonia Reinforced HDPE Biocomposites

Safieddine Bahlouli [1], Ahmed Belaadi [2,*], Azzedine Makhlouf [1], Hassan Alshahrani [3,4], Mohammad K. A. Khan [3,4] and Mohammed Jawaid [5]

1 Abbes Laghrour University, Khenchela 40000, Algeria
2 Department of Mechanical Engineering, Faculty of Technology, University 20 Août 1955-Skikda, El-Hadaiek Skikda 21000, Algeria
3 Department of Mechanical Engineering, College of Engineering, Najran University, Najran 1988, Saudi Arabia
4 Scientific and Engineering Research Centre, Deanship of Scientific Research, Najran University, Najran 1988, Saudi Arabia
5 Laboratory of Biocomposite Technology, Institute of Tropical Forestry and Forest Products (INTROP), Universiti Putra Malaysia, Serdang 43400, Selangor, Malaysia
* Correspondence: ahmedbelaadi1@yahoo.fr or a.belaadi@univ-skikda.dz

Abstract: In this research work, we aim to study the effect of the incorporation of vegetable fiber reinforcement on the thermo-mechanical and dynamic properties of a composite formed by a polymeric matrix reinforced with cellulosic fibers with the various Washingtonia fiber (WF) loadings (0%, 10%, 20%, and 30% by wt%) as reinforced material in high-density polyethylene (HDPE) Biocomposites to evaluate the optimum fiber loading of biocomposites. In addition, several characterization techniques (i.e., thermogravimetric analysis (TGA), differential scanning calorimetry (DSC), dynamic mechanical analysis (DMA), and thermal mechanical analysis (TMA)) were used to better understand the characteristics of the new composites prepared. With these techniques, we managed to verify the rigidity and thermal stability of the composites so elaborated, as well as the success of the polymer and the structural homogeneity of the obtained biocomposites. Hence, the biocomposite with the best ratio (HDPE/20WF) showed a loss modulus (E″) of 224 MPa, a storage modulus (E′) of 2079 MPa, and a damping factor (Tanδ) of 0.270 to the glass transition (Tg) of 145 °C. In addition, thermomechanical analysis (TMA) of the biocomposite samples exhibited marginally higher Ts compared to the HDPE matrix. The best results were recorded with biocomposites with 20% WF, which showed better thermal properties. This composite material can be used as insulation in construction materials (buildings, false ceilings, walls, etc.).

Keywords: Washingtonia fiber; HDPE; thermal stability; DSC/TGA; DMA; TMA

Citation: Bahlouli, S.; Belaadi, A.; Makhlouf, A.; Alshahrani, H.; Khan, M.K.A.; Jawaid, M. Effect of Fiber Loading on Thermal Properties of Cellulosic Washingtonia Reinforced HDPE Biocomposites. *Polymers* **2023**, *15*, 2910. https://doi.org/10.3390/polym15132910

Academic Editor: Łukasz Klapiszewski

Received: 3 June 2023
Revised: 28 June 2023
Accepted: 29 June 2023
Published: 30 June 2023

1. Introduction

Recently, due to the growing concern for environmental protection and sustainable development, the field of bio-based materials has taken a step forward. As experience has shown that reinforcing polymers with synthetic fibers causes serious problems, namely disposal and recycling, researchers have focused on this topic to find solutions that meet the global trends in environmentally friendly materials [1]. To solve this problem, researchers aim to prepare fully or partially biodegradable composites by replacing synthetic fibers (carbon, glass, etc.) used as reinforcement with natural fibers. These last natural fibers are recognized by their abundance, lightness, low energy consumption, biodegradability, strength, and high specific modulus. With such characteristics, vegetable fibers can be a sustainable solution for creating nature-friendly biocomposites. [2].

Due to the fight against the release of carbon into the environment and the increasing demand for clean energy production and sustainable materials with high performance for use in high-tech engineering applications, composites based on a polymer matrix reinforced

with plant fibers are attracting increasing interest. These composites offer great potential in various fields (sports, automotive, buildings, aerospace, prostheses, etc.) where the mastery of certain properties such as strength and lightness is really required [3–5]. For example, major automobile manufacturers have begun using biocomposite materials reinforced with plant fibers in vehicle interiors, such as roofs, trunk liners, internal engine covers, dashboards and door panels, sun visors, seat backs, and bumpers. As a result of their lower environmental impact, higher quality features, and possible lower production costs, biofiber/filler-reinforced polymer biocomposites have emerged as a prospective alternative to conventional composites [6–8].

The selection of a matrix plays a crucial role in mechanical characterization. There are two types of matrices that are most commonly used, namely thermoplastics and thermosets. In-depth research has been conducted on thermoplastic resins, including polyvinyl chloride (PVC), polypropylene (PP), and polyethylene (PE), to evaluate their mechanical and thermal properties [9,10]. Similarly, studies have been conducted on epoxy and polyester [11]. Indeed, plant fibers have been used by many researchers to reinforce polymer matrices, and investigations have been carried out to assess their mechanical and thermal characteristics [12–14]. These works revealed that plant fibers have the potential to improve the mechanical properties of polymer biocomposites, such as tensile strength, stiffness, and impact resistance. Moreover, plant fibers exhibit notable thermal behavior, including low thermal conductivity and high specific heat capacity. Therefore, they have established themselves as a promising alternative to synthetic fibers for reinforcing polymer matrices. Furthermore, natural fibers are abundant, renewable, biodegradable, and cost-effective, making them environmentally friendly and sustainable materials for biocomposite manufacturing [2,15].

Furthermore, the introduction of fillers can cause changes of different magnitudes in the molecular and microscopic properties of the polymer matrix. Polypropylene, a basic type of polyolefin, has attractive characteristics, including a lower cost, a wider heat treatment range, resistance to various chemicals, and thermo-oxidative stability. In addition, examining and verifying the qualities and effectiveness of composites made with natural fillers is essential, particularly when these composites experience recurring strains such as damping. DMA is a widely used method to study these characteristics by subjecting composite materials to a sinusoidal force and observing how they react with temperature change, frequency, and time. The polymer modulus is categorized into E' and E''. When the temperature rises, the E' of polymers tends to decrease, while the E'' and Tanδ increase until they reach the Tg. The rigidity of the specific polymer composite is recognized as the cause of the decrease in E', whereas E'' corresponds to the energy dissipation caused by the viscous phase of the polymer [16].

The research work by K. Senthilkumar et al. [15] analyzes the effect of fiber loadings (between 25 and 45 wt%) and different treatments (NaOH and KOH) on the thermomechanical and dynamic properties of biocomposites made of pineapple leaf plant fibers/polyester (PALF/PE). The recorded results demonstrated that composites reinforced with treated fibers had a higher compressive strength and storage modulus than composites filled with virgin fibers. In addition, TMA analysis showed that biocomposite reinforced with 45% fiber exhibited the least dimensional change, signifying better dimensional stability.

The study, led by Saba et al. [17], conducted a comparison between different hybrid nanocomposites (oil palm nanofillers/epoxy and kenaf/epoxy) and analyzed the dynamic mechanical properties. The reinforcement of 1.0 wt.% of oil palm nanofillers improved the E' and E'' while reducing damping properties. The hybrid nanocomposites also exhibited a higher Tg of 81 °C with a peak height of Tan δ of 0.36. The study suggests that oil palm nanofillers can enhance the dynamic mechanical properties of kenaf/epoxy composites. Asim et al. [18] have studied the influence of fiber loading (40–60 wt.%) and silane treatment (concentration of 2% for 3 h) on the thermal and dynamic properties of PALF and KF composites. Results showed that increasing fiber loading led to an increase in glass transition Tg temperature while thermal stability decreased. In addition, fiber treatment

improved thermal stability and reduced flammability. According to the DMA results, the E′ of pure phenolic was found to be the lowest. However, when PALF was added to the phenolic composite at percentages ranging from 40% to 60%, the E′ increased for the composite containing untreated and treated 50% PALF and 50% KF. This increase in E′ can be attributed to the rigid properties of the KF reinforcement. Another recent research work carried out by Asim et al. [19] on the same date palm fiber (DPF) studied the effect of DPF loading ratio on the thermo-mechanical properties of phenolic composites. Results showed that as the fiber loading increased, the mechanical properties increased while the thermal stability decreased. The maximum tensile strength and modulus were achieved with 50% fiber reinforcement. Moreover, the addition of DPF improved the impact strength of the biocomposites. The study highlights the low values of Tanδ for the composites made from DPF. However, an increase in the fiber loading leads to an increase in the Tg of the damping factor. Based on the results, it can be deduced that the composites made with a 50% DPF filler have improved thermomechanical properties due to the good adhesion of the fibers within the polymeric matrix and in the interfacial region. Therefore, this material can be a promising candidate for insulation applications in buildings. In another study, Asim et al. [20] investigated the thermomechanical and dynamic properties of kenaf/PALF/phenolic biocomposites. The composites were produced using hot pressing and varying amounts of kenaf and PALF fibers. Indeed, out of all the hybrid biocomposites, the 15%-PALF/35%-kenaf hybrid biocomposites demonstrated the highest values of E′ at 55 °C and E″ at 101 °C. The minimum Tanδ peak intensity was recorded at 128 °C, while the biocomposite hybrid 35%-PALF/15%-kenaf showed a maximum Tanδ peak intensity at 137 °C. Recent work by Shaikh et al. [21] explored the effects of adding date palm nanofiller to PP on its dynamic and thermo-mechanical properties (DMA and TMA). Dynamic mechanical analysis showed enhanced E′ and Tg temperatures. When compared to PP in its solid state, the biocomposites exhibited a decrease in both E′ and E″ with increasing temperature. At 50 °C, the difference in E′ between the biocomposites and PP was only 9%. Conversely, in the melt state, there was an increase in E′ and E″ across the entire range of angular frequencies. The E′ of the biocomposite containing 1 wt% nanofiller was measured at 0.85 MPa, while the E′ of PP at 0.1 rad/s was 0.732 MPa. According to the authors, developed nano-biocomposites exhibit remarkable dimensional stability in a well-defined temperature and frequency range in the solid state while showing the identical viscoelastic behavior of a mixed polymer liquid in the molten state. Another study conducted by Jawaid et al. Jawaid et al. [22] aim to improve the thermal behavior of epoxy hybrid biocomposites loaded with DPF (short fibers 0.8–1 mm) and bamboo fibers (BF). The authors showed that the performance of the hybrid biocomposite was similar to that of a composite made from BF. Moreover, the analysis of natural fibers derived from different regions of the date palm tree revealed that, when compared to BF, these fibers considerably enhanced the thermal stability and thermo-mechanical properties. The use of hybridized fibers in the epoxy-reinforced biocomposites resulted in improved dynamic mechanical properties, surpassing those of single-fiber composites without hybridization. Gheith et al. [23] investigated the influence of plant fiber loading (40%, 50%, and 60% by weight) in the epoxy matrix on the thermal, flexural, mechanical, and dynamic properties of DPF-reinforced epoxy biocomposites. The results demonstrated that incorporating DPF significantly enhanced the flexural strength (32.6 MPa) and modulus (3.28 GPa) of the biocomposite when loaded with 50% DPF. Moreover, the composite showed improved thermal stability with a degradation temperature, and DMA indicated an increase in E′, E″, and Tg, but the 50% DPF loading showed a net improvement compared to the 40% and 60% DPF charges. Sreenivasan et al. [24] have examined the dynamic mechanical and thermal properties of Sansevieria cylindrica/polyester composites, focusing on the effects of fiber length, loading, and different chemical treatments. The results illustrated that the increase in both factors (fiber length and loading) improved the E′ and Tg of the biocomposite. Chemical treatment further enhanced the dynamic mechanical properties. TGA showed improved thermal stability. Khan et al. [25] examined the impact of cellulose nanofibers and

nanoclays (montmorillonite and organoclay) on the mechanical, morphological, thermal stability, and dynamic mechanical properties of kenaf fibers/epoxy nano-biocomposites. The incorporation of CNFs and nanoclays (MMT) resulted in improved tensile strength by 103% and 50%, respectively. CNFs also increased flexural strength by 23.5% and storage modulus by 26%, while nanoclays decreased a damping factor (Tan δ) by 30%. The study demonstrated the potential of CNFs and nanoclays as effective reinforcements for kenaf/epoxy composites.

The purpose of this work is to characterize the thermal properties of previously developed systems (reinforced HDPE not treated with different fiber loads). For that, we used different techniques: the thermogravimetric analysis TGA, to determine in particular the temperature of maximum degradation of our systems; the differential scanning calorimetric analysis DSC, to evaluate the rate of crystallinity and the temperatures of transitions of first order (fusion T_f) and second order (glass transition T_g); the dynamic mechanical analysis DMA, to differentiate the phenomena of relaxation and to study the properties; and finally, the thermomechanical analysis TMA. On the other hand, the damping characteristics that are in high demand in various applications, namely automotive components and the development of light structures, are explored through DMA and free vibration.

2. Experimental Procedure

2.1. Fiber Extraction and Preparation

The Washingtonia filifera (WF) plant, also known as the desert palm or California palm, is a flowering plant endemic to the southwestern United States and Baja California. This plant can grow up to 15 to 20 m tall and 1 to 4 m wide and has a stout, cylindrical trunk with waxy, fan-shaped leaves. However, it is easily cultivated locally in the region of Skikda (Algeria). Indeed, the natural fibers of WF are easy to remove from the leaf because they are visible to the naked eye. After being removed by hand, the fibers are cleaned. In order to increase the matrix-fiber adhesion and mechanical capabilities, the fibers are properly treated with distilled water (immersed for 20 min at 60 °C), washed with distilled water, and dried in an oven at 65 °C for 20 min to remove the impurities stuck in the fiber surface and generate high-quality fibers. The Washingtonia fibers were dried in an oven at 80 °C for 2 h before being incorporated into the HDPE matrix.

2.2. Thermoplastic Matrix

In this work, we used samples of HDPE (high density polyethylene), which is a semi-rigid plastic with a linear structure, supplied by the company SABIC Petrochemicals under the reference PPC10642 (purity = 95%, average density of 0.96, and MFI of 0.4). The molecular weight of the HDPE used is 300,000 g/mol.

2.3. Elaboration of HDPE/WF Biocomposites

The biocomposite was created using a rolling process with two Thermotron-C. W. Brabender model T303 rouleaux at a temperature of 165 °C for 15 min. To begin, 20% of the weight of HDPE was melted on the rouleaux at 175 °C for 12 min. The WF fibers were then cut between 2 and 5 mm, and the remaining HDPE was added and mixed for 8 min at 65 rpm. The biocomposite was then mixed five to six times for 5 min to improve the homogeneity of the material. Finally, the biocomposite was removed from the rollers and cut to the size of the selected mold. The samples were processed in a mold that was maintained at a temperature of 190 °C for 5 min using a Dake press at a pressure of 10 MPa, and at the end the mold was cooled to 50 °C with cold water (Figure 1). Many formulations developed in this study are cataloged in Table 1.

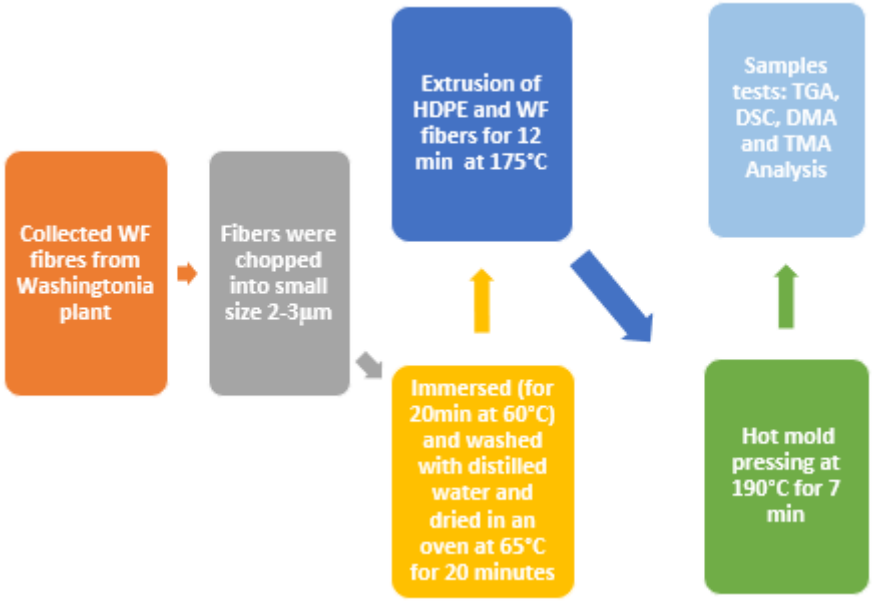

Figure 1. Flowchart of different steps for HDPE-WF biocomposite preparations and tests.

Table 1. Codification of composition elaborated in this work.

Reference Name	Washingtonia Fibers (wt.%)	HDPE (wt.%)
HDPE	0	100
HDPE-10WF	10	90
HDPE-20WF	20	80
HDPE-30WF	30	70

2.4. Thermal Analysis

2.4.1. DSC

The DSC objective is to identify the differential in heat flow established between a sample (E) and a reference (R) while heating or cooling by keeping their temperatures constant. This heat flow is proportional to the heat capacity of the substance under consideration. Whether an endothermic or exothermic event happens during the scan, the flux varies, resulting in a peak on the DSC thermogram. In fact, this approach can be used to study the effect of fiber insertion on the thermal characteristics of the matrix. The heat balance is thus expressed as Q = m Cp ΔT, where Q represents the amount of heat exchanged in joules (J) and m represents the sample's mass in grams (g). ΔT: difference of the temperature in K; Cp: heat capacity (J/g·K). With an apparatus type Shimadzu DSC-60, we performed thermal studies on the various materials (HDPE and HDPE/WF). A sample amount of 11 to 13 mg was weighed and placed in a sealed aluminum capsule before being placed in the oven. The entire analysis cycle begins with a temperature rise from 25 °C to 200 °C to erase the material's thermal history, followed by a decline from 200 °C to 25 °C before another rise to 200 °C. The scans (heating and cooling rates) are carried out at 10 °C/min with a nitrogen (N_2) gas flow of 50 mL/min. The endothermic peak was used to determine the crystalline melting temperatures (T_m) and the crystallinity ratio (Xcr) of the studied samples. A reference value of $\Delta H^0_{f-HDPE} = 281 \frac{J}{g}$ [26] for the enthalpy of crystallization of 100% crystalline polyethylene was used.

2.4.2. TGA

Thermogravimetry is a thermal analysis commonly used to determine the thermal stability of natural reinforced fiber polymers. In addition, it studies the variation of the mass of a substance as a function of time or temperature. This technique is generally

applied to study certain thermal phenomena such as adsorption, desorption, vaporization, decomposition, oxidation, and reduction [27]. TGA analyses were performed by Shimadzu DTG-60H equipment, with the microbalance having an accuracy of ±0.1 µg. Samples of approximately 11 to 13 mg were placed in 70-microliter alumina molds. To characterize the thermal stability of the biocomposites. The samples were heated at 10 °C/min from 25 to 200 °C under a controlled nitrogen atmosphere, and the flow rates were 50 mL/min and 20 mL/min, respectively. Indeed, the peak degradation temperature (T_{deg}) represented the temperature at which the rate of degradation was maximal.

2.4.3. DMA

Dynamic mechanical analysis consists of measuring the response of a material following a dynamic loading as a function of frequency and temperature and is also related to the development of the viscoelastic behavior of polymeric and composite materials. It provides useful information on the conservation (E′) and loss (E″) moduli as well as the tangent of the loss angle Tanδ (loss factor: Tanδ = E″/E′). Indeed, E′ represents the stiffness and the elastic component of the material. The loss modulus E″ represents the viscous component of the material. The viscosity indicates its capacity to dissipate mechanical energy. This behavior is related to the friction of the chains of molecules and their flow, and finally, the loss factor corresponds to the fraction of energy dissipated in viscous form. During our work, we used the NETZSCH DMA-242E ARTEMIS device. The measurement conditions are: 2 °C/min, 25 to 180 °C, and 1 Hz for heating rate, temperature range, and frequency, respectively, with nitrogen as the sweep gas. The HDPE/WF and HDPE samples for DMA in 3-point bending mode have a geometry of 40 × 10 × 2.2 mm^3.

2.4.4. TMA

The Perkin Elmer TMA-7 apparatus was used to determine the melting temperature (T_m) and softening temperature (T_s) of pure HDPE samples and HDPE/WF biocomposites. The samples, which measured 5 mm (length) × 5 mm (width) × 2.2 mm (height), were tested under a nitrogen gas atmosphere (50 mL/min) and an applied force of 5 mN using a penetration probe mode. The tests were conducted in a temperature range of 25 °C to 200 °C with a heating rate of 5 °C/min, and refrigerated cooling was also applied. The results were processed using Pyris v12.1 software.

3. Results and Discussion

3.1. TGA Analysis

As described in Section 2.4.2, thermogravimetric analysis allows one to monitor the variation in mass of a sample as a function of temperature and thus access the decomposition parameters of the biocomposite. To facilitate reading, it is convenient to represent the TGA curve of the mass loss in % as a function of temperature in °C. Figure 2 shows the thermogravimetric behavior (TGA) of HDPE and HDPE-WF at different Washingtonia fiber loadings (10, 20, and 30% fiber) for a heating rate of 10 °C/min with an N_2 atmosphere over a temperature range of 20 °C to 600 °C in order to track their thermal behavior (refer to Table 2). The graph (Figure 2) makes it possible to monitor the thermal behavior of the samples under study and subsequently discuss the effect of incorporating the WF reinforcement into the HDPE matrix on the thermal stability of the resulting biocomposites. The parameters that could account for thermal stability are the initial degradation temperature, the major degradation temperature, the final degradation temperature, and the amount of char formation. Each TGA curve shows two distinct regions of degradation for all biocomposites. The TG curves show that the degradation of HDPE occurs in a single step and starts at 496 °C and ends at a temperature of 518 °C [28]. In contrast, the blend biocomposites reveal that Washingtonia fibers decompose throughout the process, while HDPE begins to decompose at a temperature of 396 °C and experiences the highest rate of weight loss at 480 °C. The TG curve for HDPE indicates that volatile emission begins at 415 °C, and the maximum weight loss rate is recorded at 518 °C. In fact, in all the bio-

composites (HDPE-10WF, HDPE-20WF, and HDPE-30WF), the initial degradation occurs within the temperature range of 100–250 °C. This is primarily due to the evaporation of physically weak water molecules on the biocomposites' surface and dehydration caused by the secondary alcoholic groups [29]. According to the TGA graph, in the case of HDPE-WF composites, the curves demonstrate a two-stage degradation process. The first stage, which takes place between 241 and 378 °C, is attributed to the degradation of WF fibers [28]. Conversely, the primary step involving the degradation of the HDPE matrix occurs in the temperature range of 391–492 °C. The degradation range of lignocellulosic materials typically falls within 150–500 °C. Cellulose exhibits thermal stability within the range of 275 °C to 500 °C, whereas hemicellulose and lignin have degradation ranges of 150–350 °C and 250–500 °C, respectively [30].

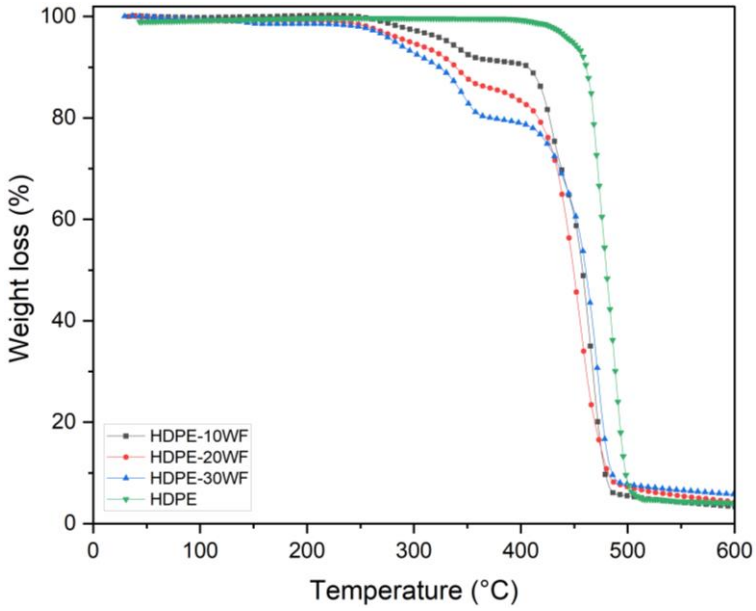

Figure 2. TG curve for different HDPE-WF biocomposites prepared in this work and HDPE.

Table 2. TGA results of samples elaborated in this study.

Materials	First Degradation Stage (°C)	Second Degradation Stage (°C)	T (°C) at 10% of Weight Loss	T (°C) at 50% of Weight Loss	Residue (%) at 600 °C
HDPE	396–518	/	459	481	3.98
HDPE-10WF	256–375	398–499	404	460	3.52
HDPE-20WF	241–378	391–492	337	458	5.17
HDPE-30WF	248–389	389–501	323	451	7.01

Table 2 indicates that weight loss occurs beyond 500 °C, resulting in the breakdown of hydrogen bonds within aromatic polyamides and leading to complete decomposition of the fibers and polymer. The largest amount of residue is shown with the HDPE-30WF and HDPE-20WF biocomposites (7.01% and 5.17%, respectively, at 600 °C). This residue is the result of the thermal degradation of hemicellulose and lignin from cellulose, which resulted in char formation.

3.2. DTG Analysis

For ease of reading, it is convenient to plot the derived curve DTG of the TGA. This curve makes it easier to identify mass loss phenomena since they are presented as peaks. However, we lose an essential piece of information: the residual mass of the sample at the end of the experiment. Figure 3 shows the behavior of the first derivative of the

thermogravimetric TGA curve of HDPE and a comparison of the three biocomposite systems developed in this work. As depicted in Figure 3, better thermal stability of HDPE-WF biocomposites is achieved with a WF fiber reinforcement ratio of about 10% by mass. It should be noted that after this level of reinforcement, the thermal stability of the biocomposite drops, which is why the melting temperature of the HDPE-30WF biocomposite is much lower than that of HDPE (see Table 2).

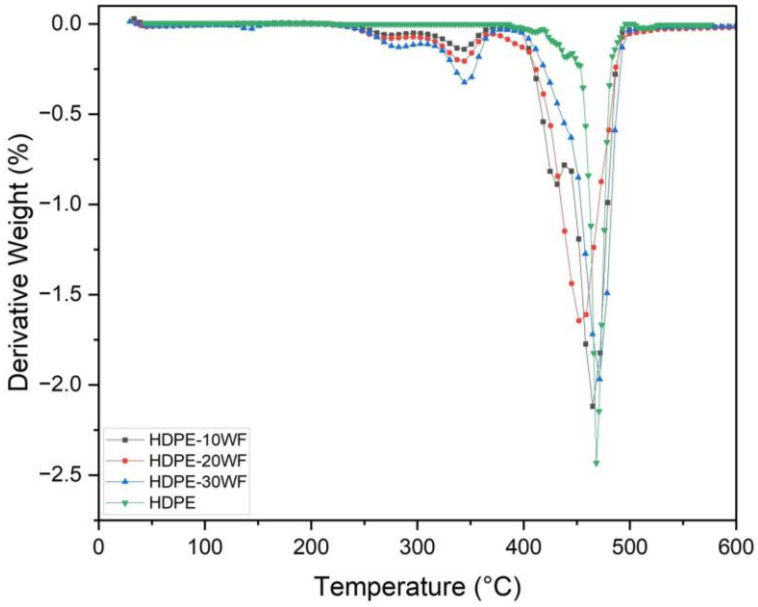

Figure 3. Derivative weight in % as a function of temperature for different HDPE-WF biocomposites and HDPE.

In the case of biocomposites with 30% reinforcement, the DTG curves do not correspond to what would be obtained by adding the partial contributions of each constituent (Washingtonia fibers and HDPE) since there is a temperature shift. We observe: (i) a low-intensity peak at T = 361 °C, which corresponds to fiber degradation. This shift towards lower temperatures indicates reduced thermal stability of the fibers. This variation is not due to the association with HDPE. It is essential to recall that the fibers in the composite material have already undergone many mechanical and thermal stresses during mixing. (ii) a high-intensity peak at 462 °C, shifted to a higher temperature region than that of the matrix (459 °C), which corresponds to HDPE chain degradation. Consequently, many studies [31] show that beyond 500 °C, polymer chains are completely degraded. In our case, we observe that its decomposition begins around 400 °C and continues until reaching the maximum decomposition temperature of 485 °C. At this temperature, the polymer chains are completely degraded. The decomposition is fully completed beyond 500 °C, and the residual mass represents only 7% of the initial mass in the 30% fiber composite.

3.3. DSC Analysis

Melting is a phenomenon where solid and liquid phases coexist in equilibrium. It corresponds to a constant physical characteristic for each polymer. During melting, crystals absorb energy (an endothermic phenomenon), and this energy corresponds to the enthalpy of fusion (ΔH_f). The polymer crystallinity ratio $\chi_r(\%)$ is determined by its melting enthalpy. The expression to estimate it is $\chi_r(\%) = 100 \times (\Delta H_m/(1-X) \times \Delta H)$. Or ΔH: specific enthalpy of fusion of the perfect crystal (value from literature) and ΔH_m specific enthalpy of fusion of the polymer, determined by integration of the peak of fusion for the polymer. In the case of composites, the mass fraction of the polymer is equal to (1 − X), where X is the fiber ratio. It is therefore necessary to correct this value by the polymer fraction. The DSC analysis was performed according to the conditions detailed in the section

dedicated to materials and methods. Figure 4 shows the thermogram of the HDPE and HDPE-WF biocomposites matrix during the temperature rise from 25–200 °C. The curve shape shows that it is a semi-crystalline polymer composed of a single α-crystalline phase. The heat flux evolution shows a single endothermic melting peak (T_m = 144 °C). The same thermogram profile is observed for both raw and processed fiber-reinforced composites. Table 3 presents a summary of the DSC measurements that determined the melting and crystallization behavior of the materials. The results indicate that the crystalline melting temperature of the HDPE matrix in the composites was lower than that of pure HDPE. Furthermore, the T_m values of the composites decreased as the fiber content increased, as indicated in Table 3. This phenomenon could be explained by the strong nucleation that occurred on the fiber surfaces, which reduced the time required for HDPE crystallization. The melting temperatures (T_m = 144, 140, 136, and 136 °C) of all tested samples decreased, and the percent crystallinity of HDPE (%χ_r) significantly increased (28.18%, 29.04%, 32.02%, and 39.48%) when reinforced with Washingtonia fibers. This indicates that the fibers have a strong ability to act as heterogeneous nucleating agents [32]. To evaluate the impact of Washingtonia fiber reinforcement on the crystallization behavior and thermodynamics of the HDPE matrix, the thermal crystallization of pure HDPE and its composites was analyzed in the temperature range of 25–200 °C. Furthermore, the addition of WF fiber reinforcement to HDPE improves the thermal stability of HDPE-WF biocomposites, with a saturation ratio of up to 20 percent by mass. Indeed, it is confirmed that HDPE-30WF biocomposite melts at a much lower temperature than HDPE. The biocomposite so generated can be used in a wider variety of contexts, provided that a loading ratio of up to 20% by mass of WF is maintained [33].

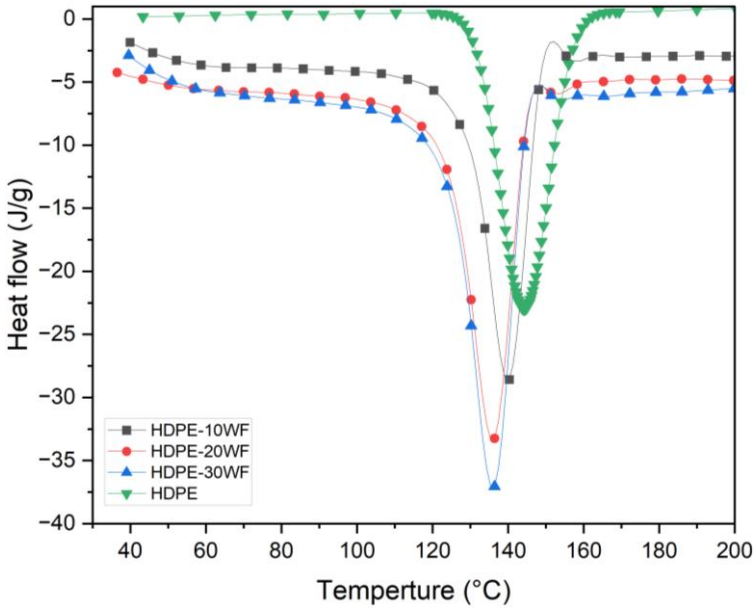

Figure 4. DSC curves for different HDPE-WF biocomposites and HDPE.

Table 3. DSC results of samples elaborated in this study.

Materials	T_m (°C)	T_{onset} (°C)	T_{offset} (°C)	ΔH_m (J/g)	X_r (%)
HDPE	144	123	165	81.16	28.18
HDPE-10WF	140	106	155	76.33	29.04
HDPE-20WF	136	103	148	92.13	32.02
HDPE-30WF	136	102	148	97.67	39.48

3.4. DMA Analysis

The DMA test enabled the acquisition of values for parameters such as E′ and Tanδ. Various factors, including the type of resin, reinforcement, and resin interfaces, as well as the interfacial region between them, can impact the viscoelastic properties of composites. Furthermore, the addition of fillers can affect the modulus of polymeric matrix composites. DMA serves as a useful method for analyzing the structural and viscoelastic behavior of materials, with a particular focus on primary relaxations, crosslinking, and density [34]. The E′ obtained from DMA can be correlated with the Young's modulus and stiffness of the composite material [35]. In addition, the applied energy generates the dissipation of thermal energy, which is related to the E″ [36], and the damping factor, or Tanδ, tells us about the internal friction and provides insight into the internal friction and molecular motion of the materials [36,37]. In this study, DMA was used to evaluate the impact of Washingtonia particles (WP) on the viscoelastic response of HDPE in the solid state.

3.4.1. Storage Modulus E′

The temperature-dependent E′ graph tells us about the stiffness, the interfacial bonding between the fibers and the matrix in the materials, and the degree of cross-linking [36]. E′, which reflects a polymer material's load-bearing capacity and stiffness, represents the elastic energy accumulated during one oscillation cycle, as previously reported [37,38]. E′ can be divided into three parts: the first is the glassy phase, followed by the transition phase, and lastly the rubbery phase. The first region corresponds to the freezing state, which is very immobile, compact, and tightly packed with the constituents of the composite material [18]. The transition region represents the stage where the storage modulus curve drops after passing through the glass transition temperature (T_g), as shown in Table 4, due to an increase in polymer chain mobility above T_g [39,40]. Finally, the rubbery region corresponds to a temperature range that causes the material to become more structurally relaxed without any other changes [41]. Storage modulus is generally correlated with Young's modulus and is largely indicative of a compound's stiffness, which determines whether a sample is considered stiff or flexible and its tendency or ability to store applied energy for later use [42]. The effect of WP on the storage modulus of HDPE biocomposites (i.e., HDPE, HDPE-10WF, HDPE-20WF, and HDPE-30WF) is presented in Figure 5, and the respective values are listed in Table 4. The results indicate that the E′ of the HDPE biocomposites increased with increasing WP content, with the highest value observed in the biocomposite reinforced with 30% WP. However, the E′ of this biocomposite decreased rapidly with increasing temperature, which can be attributed to the high-density polyethylene matrix's complex structure and high degree of polymerization. Although initially displaying a lower E′ compared to the composites, the matrix transitioned into the rubbery region as temperature increased, resulting in increased polymer mobility and flow and a reduced reinforcing effect of the fiber on the polymer chain [19]. Asim et al. [18] and Ramakrishnan et al. [43] suggest that a higher E′ value in a sample indicates increased stiffness, as it restricts the movement of matrix chains and enhances bonding between the reinforcement and matrix. The incorporation of particles was found to slightly improve the E′ of HDPE. However, at 150 °C, which is the rubbery region, both HDPE-10WF biocomposites and HDPE showed a lower E′ value. As the temperature increased, the increase in free volume and molecular mobility caused a decrease in E′, with molecules absorbing more energy, resulting in large-scale conformational rearrangements [2]. Although there were no significant differences in E′ observed for HDPE-20WF and HDPE-30WF biocomposites at higher temperatures (rubbery region), E′ was mainly dominated by the intrinsic matrix modulus [44,45]. Previous studies have also shown comparable patterns in the viscoelastic characteristics of natural fiber-reinforced polymers [21,36,46], such as in the cases of PP/date palm nanofiller, PP/yerba mate residues, and treated kenaf-pineapple fibers/phenolic. However, several other aspects, including the structure of the matrix and the nature and amount of fiber present as reinforcement with specific orientations, the appropriate chemical treatment, and the size of the fibers, will likely have a significant effect on the final properties of

biocomposites. The temperature-dependent behavior of the biocomposite can be observed in Figure 5, where it is apparent that the E′ values decrease as temperature increases. This decline is due to the biocomposite transitioning from the glassy region to the rubbery region. Within the glassy region, the biocomposites exhibited E′ values in the following order: HDPE-30WF > HDPE-20WF > HDPE-10WF > HDPE. Additionally, Figure 5 reveals that the untreated HDPE-WF biocomposites had the highest E′ peak when the fiber loading was 30 wt%. This result aligns with previous studies [47–49], which have also found that E′ peaks at higher fiber loadings. The incorporation of a higher amount of cantante fibers in the polymer resulted in increased stiffness at higher temperatures, as shown by the E′ values of HDPE-WF biocomposites in a temperature range that starts at 50 °C and stops at 100 °C, as per Figure 5. Table 4 indicated a rise in E′ (2211 MPa) at 30 wt% of cantante fibers, owing to improved stress transfer from the fiber to the matrix with a higher fiber loading. However, the value of HDPE-10WF was found to be 1812 MPa. These findings were consistent with the outcomes reported by Indira et al. [50], who used banana fibers as reinforcements for a biocomposite made with a phenol-formaldehyde matrix.

Table 4. DMA results obtained for HDPE matrix and HDPE/WF biocomposites.

Materials	Storage Modulus		Loss Modulus		Tan δ Peak	
	E′ (MPa)	Tg Value (°C)	E″ (MPa)	Tg Value (°C)	Tan Delta	Tg Value (°C)
HDPE	1642	31.52	180	48.63	0.23	113.11
HDPE-10WF	1812	34.16	201	50.11	0.234	122.14
HDPE-20WF	2079	37.49	224	51.92	0.270	145.95
HDPE-30WF	2211	35.07	246	49.43	0.239	139.47

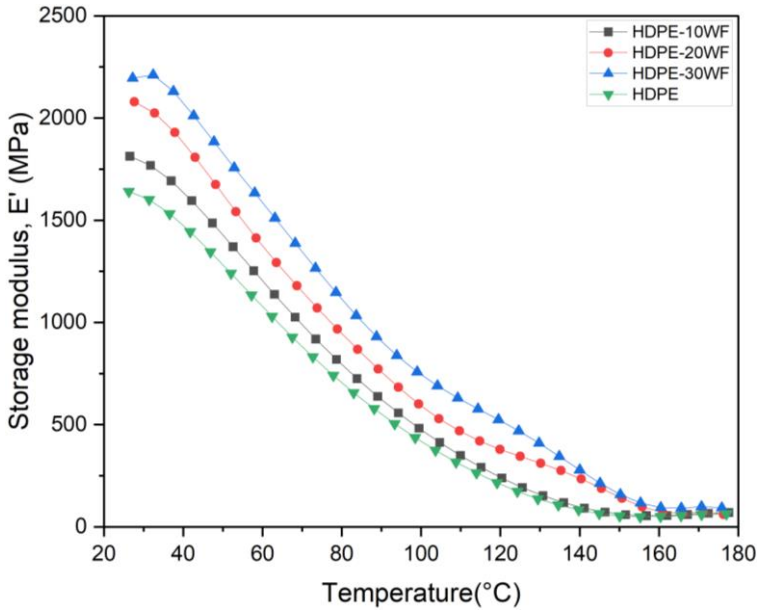

Figure 5. E′ curves for different HDPE-WF biocomposites and HDPE.

3.4.2. Loss Modulus E″

The loss modulus E″ is a measure of the energy released by a material in response to sinusoidal loading as a function of temperature [51]. It reflects the damping or viscous properties of the material and indicates the amount of energy dissipated due to molecular mobility. As shown in Figure 6, the E″ of HDPE-WF biocomposites was higher at 30 wt%, indicating increased energy dissipation in the biocomposites due to the addition of fibers. The fiber/matrix interaction in the biocomposites is improved by the addition of fibers, resulting in larger energy dissipation. The E″ values increased in the order

HDPE-30WF > HDPE-20WF > HDPE-10WF > HDPE, indicating that the addition of more fibers led to higher energy dissipation. The treatment of the fibers enhances the interfacial bonding between the fiber and matrix, reducing the molecular mobility of the polymeric chains and providing good frictional resistance, leading to higher energy dissipation and greater E″ for composites with treated fibers. This effect has been demonstrated by several researchers, such as in the case of *Sansevieria cylindrica*/polyester [24] and oil palm fibers/linear low-density polyethylene (LLDPE) matrix biocomposites [52].

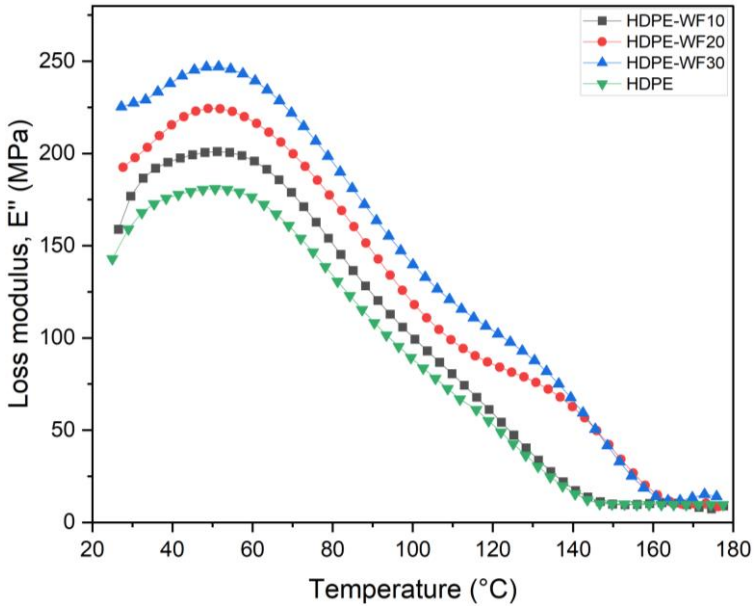

Figure 6. E″ curves for different HDPE-WF biocomposites and HDPE.

The graph in Figure 6 demonstrates the temperature-dependent behavior of E″ for HDPE-WF biocomposites and HDPE. The E″ value for HDPE-30WF biocomposites was found to be higher (224 MPa) than that for HDPE-10WF biocomposites, which showed the lowest E″ peak (201 MPa). Furthermore, HDPE-20WF biocomposites showed the highest E″ value in the glass transition region T_g, followed by HDPE-10WF and HDPE-30WF biocomposites, with values of 51.92 °C, 50.11 °C, and 49.43 °C, respectively. Above 140 °C, the E″ values of HDPE-WF biocomposites appeared to be similar for 20% and 30% loadings, likely due to comparable molecular motions. Similar findings have been reported, indicating that composites with a higher degree of reinforcement tend to exhibit higher T_g values [53]. The low E″ value of HDPE-WF biocomposites with a 20% fiber loading could be due to the fibers stopping the polymer from moving freely, as suggested in previous studies [54]. Moreover, biocomposites containing a weight fraction of 30% WF showed a significantly higher loss modulus, and this is due to the displacement of the WF fiber saturation ratio from the HDPE matrix, which confirms the results obtained by TGA/DSC. Previous research studies [18,19,55] have also reported a similar trend wherein higher weight fractions of fibers (50 wt%) lead to greater energy dissipation due to internal friction and a wider relaxation period. It should be noted that the biocomposites with a 30 wt% loading were the only ones that showed a marginal improvement in loss modulus compared to pure HDPE. A loss modulus analysis can be used to determine the glass transition temperature of biocomposites and HDPE, as shown in Table 4. In this study, the results show that all WP-reinforced biocomposites have a nearly constant glass transition temperature. This observation is in line with the results reported in a previous study [56], which also noted that the inclusion of WP did not significantly affect the glass transition temperature. Furthermore, it is possible that the incorporation of particles within the matrix of a polymer results in a composite with a glass transition temperature almost the same as the starting polymer; this result is observed when the interaction between these particles

and the polymer matrix is sufficiently weak [17,57]. In the case where E′ > E″, there is an interconnection of the particles of the natural filler in the HDPE-WF biocomposite [58].

3.4.3. Cole-Cole Plot

The Cole-Cole plot is a valuable tool for determining the degree of uniformity or non-uniformity in filler dispersion within the polymeric matrix, which represents the homogeneity or heterogeneity of composites. Moreover, it serves as an indicator of poor interfacial bonding between fiber and matrix [59]. Additionally, this curve can be plotted to reveal the relationship between E′ and E″ [17,60,61]. The nature of the Cole-Cole mapping allows for evaluation of the viscoelastic properties and homogeneity of the studied biocomposites [22,62–64]. In addition, an irregular shape indicates poor adhesion at the interface caused by heterogeneous phase dispersion in the composite system [65]. It also allows one to determine the structural changes that take place in the cross-linked polymers after their loading by the reinforcement [66]. According to the literature, a smooth, semi-circular, arc-shaped curve is indicative of a homogeneous polymeric system [15,62,64]. Figure 7 shows the Cole-Cole plots of HDPE and HDPE-WF biocomposites, in which E″ is plotted as a function of E′. Observations from the curve indicate that all the biocomposites exhibit a perfect semi-circular shape, which is consistent with a homogeneous polymeric system. Similar behavior was observed as a perfect semi-circle by Joseph et al. [67] in the case of PP/sisal biocomposite. Conversely, various researchers have detected an imperfect semi-circular arc, which indicates heterogeneous filler dispersion in the matrix and good interfacial bonding [68,69]. For instance, basalt-aramid fiber-reinforced phenolic composites [70], ramie-glass fibers in unsaturated polyester [71], and glass/bamboo fiber-reinforced unsaturated polyester resin-based hybrid biocomposites [72] have all displayed such an imperfect arc.

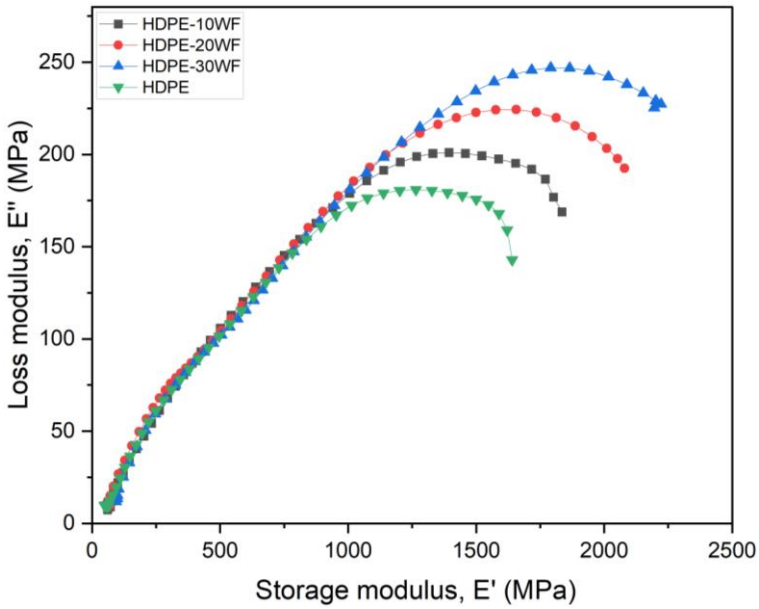

Figure 7. E″ as a function of E′ (Cole-Cole plots) for different HDPE-WF biocomposites and HDPE.

3.4.4. Damping Factor

According to the plot in Figure 8, it can be observed that the value of Tanδ increased as the temperature rose, reaching its highest point in the glass transition area before decreasing with a further increase in temperature. The damping factor declined in the rubbery phase of all the biocomposite samples with a rise in temperature, indicating a transition from the frozen stage to the mobility stage of the polymer. At the rubbery stage, the polymer or materials did not have a defined structure remaining [73]. Other studies conducted on cellulosic fibers with polymer biocomposites have reported similar trends [74–76].

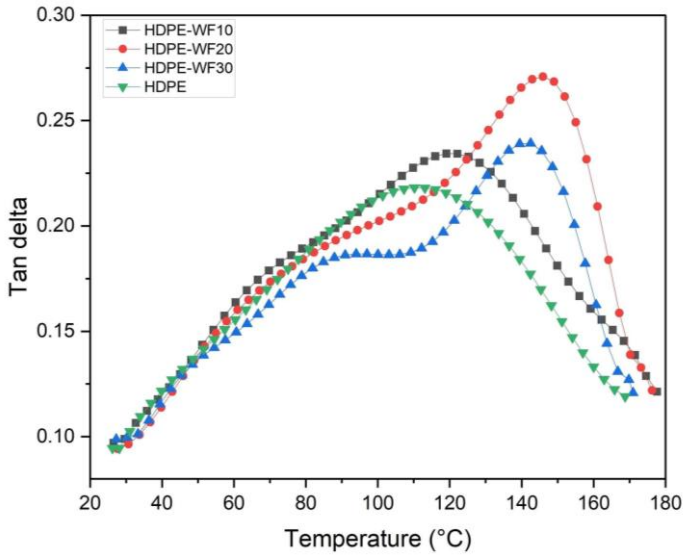

Figure 8. Tanδ curves for different HDPE-WF biocomposites and HDPE.

Table 4 and Figure 9 present the peak Tanδ and glass transition temperature values obtained from the Tanδ plots. In the case of HDPE-WF biocomposites, the highest peaks Tanδ values were observed at 20 wt% and 30 wt% loading, with values of 0.27089 (corresponding to a higher T_g of 145.95 °C) and 0.23916 (corresponding to a higher T_g of 139.95 °C), respectively. Furthermore, the Tanδ values of HDPE-WF biocomposites increased with fiber loading up to 20% and then decreased for the biocomposite loaded with 30% WF fibers (as shown in Table 4). The highest peaks Tanδ and T_g values were observed for the HDPE-20WF formulation (at 20 wt% of WF fibers), as shown in Figure 9, indicating poor fiber-matrix adhesion and increased molecular movement in the polymer chains, which result in higher damping characteristics. Conversely, a lower damping factor in the plot indicates improved interfacial adhesions between the reinforcement and polymer, as reported by other studies [62]. The glass transition temperature exhibited an increasing trend in the HDPE-10WF, HDPE-30WF, and HDPE-20WF biocomposites, with values of 145.95 °C, 139.47 °C, and 122.14 °C, respectively. Similarly, the Tanδ values of the composites followed the same pattern. The peak Tanδ value of the biocomposite system varied with the improvement of the reinforcing fibers, which can be explained by the concentration of shear stress in the fibers and the viscoelastic energy loss of the polymeric matrix. This phenomenon has been reported in previous studies [66]. A study of the dynamic mechanical characteristics of several HDPE composites reinforced with natural fibers was made, and it was recorded that a decrease in the values of Tanδ is explained by a more elastic behavior of the composites compared to the HDPE matrix [77]. The reduction in Tanδ values can be attributed to the decrease in viscoelastic lag between stress and strain [78]. The T_g obtained from the E″ curve for HDPE-20WF was 51.92 °C, which was relatively lower than the T_g obtained from the Tanδ curve (145.98 °C for the same biocomposite, as shown in Table 4). At higher temperatures (100–150 °C), the overlapping of the curves indicated that there was no effect of adding fillers on the viscous dissipation. This trend was also observed in hybrid biocomposites of glass-ramie fibers/polyester [79], glass-pineapple leaf fibers/epoxy [80], and glass-Pennisetum purpureum fibers/epoxy [81]. Generally, the Tanδ allows us to conclude that the glass transition temperature is higher than the loss modulus of 80–100 °C. As the availability of bulk fibers to dissipate vibrational energy is reduced, Tanδ values are higher in biocomposites compared to HDPE.

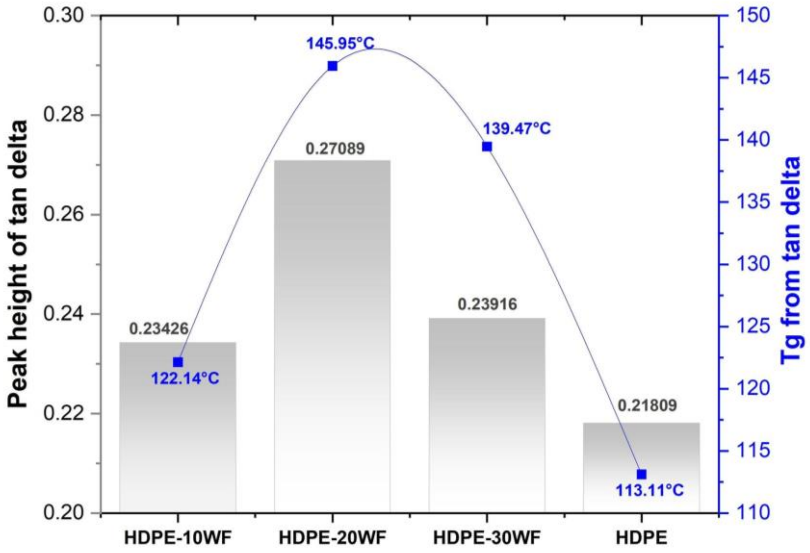

Figure 9. Peak height and T_g of HDPE-WF biocomposites and HDPE.

3.5. TMA Analysis

To determine the melt temperature (T_m) or softening temperature (T_s) of both HDPE and HDPE-WF biocomposite samples, changes in probe height (%) were analyzed with respect to temperature (25–200 °C) in the penetration mode using TMA. This method was selected due to its sensitivity and ease of use in measuring both HDPE and HDPE-WF [82] (Figure 10). T_m signifies the initial point at which the sample softens, providing valuable insight into the entanglement between the polymer matrix and the reinforcing materials [83,84]. Typically, the softening temperature increases as the formation of chain entanglements occurs [85]. The T_m of HDPE, HDPE-10WF, HDPE-20WF, and HDPE-30WF biocomposite were 132.16 °C, 137.05 °C, 139.68 °C, and 137.75 °C, respectively. The marginally elevated T_m values observed in the composites may be attributed to the interactions between the fiber and matrix, which can impact the HDPE crystalline structure [86]. As the fiber loading increased, there was a minor rise in T_m for the HDPE-WF biocomposites. However, the T_m values for both HDPE-10WF and HDPE-30WF biocomposites were comparable, indicating that the inclusion of WF particles in the matrix had minimal influence on the T_m. Furthermore, the biocomposite samples exhibited marginally higher T_s compared to the HDPE matrix. This observation may be attributed to the interactions between particles and matrix, which impact the crystalline structure of HDPE. Additionally, the introduction of WP into the biocomposite led to increased elasticity, which likely contributed to the elevated T_s values. Similar findings were observed in the context of HDPE/wood fiber composites [86].

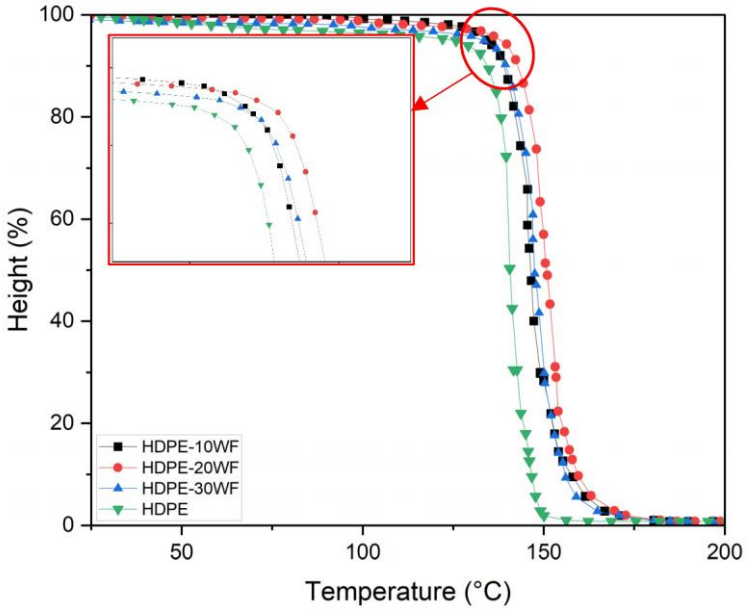

Figure 10. TMA-Height in % as a function of temperature for different HDPE-WF biocomposites and HDPE.

4. Potential Applications

The biocomposites made from WF fibers and HDPE possess excellent dynamic mechanical properties, making them a viable replacement for traditional construction materials like aluminum, steel, cement, wood, cladding, and partitioning materials in order to develop sustainable green buildings. Using these materials in construction projects can significantly reduce costs, including material costs, fabrication costs, construction costs, and repair costs.

These biocomposites have a high storage modulus and low damping factor, making them suitable for connecting bridges, stairs, bridge decks, railings, plumbing components, doors, outdoor decking, and door frames. Compared to expensive wooden blocks, they are lighter and have lower damping properties. They are also suitable for low-stress applications such as housing, windmill blades, industrial drive shafts, highway bridge support beams, and paper-making rollers. Furthermore, they have the potential to replace costly materials like stone, concrete, steel, aluminum, and timber in Algeria.

For example, the Building and Construction Division employs HDPE piping systems as ground loops for ground source geothermal applications, which are also referred to as earth energy or geo-exchange systems.

The utilization of HDPE pipes for water systems provides numerous advantages. These pipes are typically manufactured in various diameters and lengths, including straight lengths and coils. HDPE material is resistant to tuberculation and bacterial growth, making it an excellent option for use in harsh environments. Additionally, HDPE pipes exhibit superb chemical resistance properties.

5. Conclusions

The addition of Washingtonia fibers with different loadings of 0%, 10%, 20%, and 30% by wt% in a high-density polyethylene matrix resulted in the finding that the addition of WF enhanced TGA, DSC, and DTG thermograms and also improved the thermal stability of HDPE-WF biocomposites compared to HDPE. However, it should be noted that the WF saturation ratio is around 20% by mass, and at higher loads, it is noted that the melting temperature of the biocomposites shifts towards low temperatures (HDPE-30WF) compared to that of HDPE. From the TGA, it can be concluded that the formation of a significant amount of char residues is due to the thermal degradation of hemicellulose and cellulose lignin, and this is noted for the biocomposites HDPE-30WF and HDPE-20WF. According to the DTG analysis, the decomposition begins around 400 °C and continues

until reaching the maximum decomposition temperature of 485 °C. At this temperature, the polymer chains are completely degraded. The decomposition is fully completed beyond 500 °C, and the residual mass represents only 7% of the initial mass in the 30 wt% of fiber biocomposite. In addition, the DSC analysis revealed that the melting temperatures (T_m are equal to 144 °C, 140 °C, 136 °C, and 136 °C) for all samples tested decreased, and the percent crystallinity of HDPE and biocomposites ($\%\chi_r$) significantly increased (28.18%, 29.04%, 32.02%, and 39.48%) when reinforced with Washingtonia fibers. Furthermore, in the DMA analysis conducted in this study, the biocomposite material HDPE-WF, which was reinforced with 30% WP, demonstrated the highest E″ compared to the other biocomposites examined. However, as the temperature increased, the E″ of this biocomposite decreased rapidly. Additionally, an increase in E′ (2211 MPa) was noted in HDPE-30WF, which can be attributed to the enhanced stress transfer from the fiber to the matrix with increased fiber loading. Conversely, the value for HDPE-10WF was found to be 1812 MPa. The Tanδ method determined a T_g value that was higher than the loss modulus between 80 °C and 100 °C. The Tanδ values for the biocomposites were higher than those for the HDPE matrix due to a lower volume fraction of fibers available to dissipate the vibrational energy.

Author Contributions: Conceptualization, S.B., A.B. and M.J.; methodology, M.J. and A.B.; software, M.J.; validation, S.B., M.J., A.B., A.M. and H.A.; formal analysis, A.B. and A.M.; investigation, S.B., M.J., A.B. and A.M.; resources, A.B.; data curation, M.J. and A.B.; writing—original draft preparation, S.B., M.J., A.B., A.M., H.A. and M.K.A.K.; writing—review and editing, M.J., A.B., A.M., H.A. and M.K.A.K.; visualization, A.B.; supervision, A.B.; funding acquisition, H.A. All authors have read and agreed to the published version of the manuscript.

Funding: The authors are thankful to the Deanship of Scientific Research at Najran University for funding this work under the Research Groups Funding Program (grant code: NU/RG/SERC/12/24).

Institutional Review Board Statement: Not applicable.

Data Availability Statement: Not applicable.

Conflicts of Interest: The authors declare no conflict of interest.

References

1. Rangappa, S.M.; Siengchin, S.; Parameswaranpillai, J.; Jawaid, M.; Ozbakkaloglu, T. Lignocellulosic fiber reinforced composites: Progress, performance, properties, applications, and future perspectives. *Polym. Compos.* **2022**, *43*, 645–691. [CrossRef]
2. Haris, N.I.N.; Hassan, M.Z.; Ilyas, R.A.; Suhot, M.A.; Sapuan, S.M.; Dolah, R.; Mohammad, R.; Asyraf, M.R.M. Dynamic mechanical properties of natural fiber reinforced hybrid polymer composites: A review. *J. Mater. Res. Technol.* **2022**, *19*, 167–182. [CrossRef]
3. Rampal; Kumar, G.; Rangappa, S.; Siengchin, S.; Zafar, S. A review of recent advancements in drilling of fiber-reinforced polymer composites. *Compos. Part C Open Access* **2022**, *9*, 100312. [CrossRef]
4. Nurazzi, N.M.; Asyraf, M.R.M.; Khalina, A.; Abdullah, N.; Aisyah, H.A.; Rafiqah, S.A.; Sabaruddin, F.A.; Kamarudin, S.H.; Norrrahim, M.N.F.; Ilyas, R.A.; et al. A Review on Natural Fiber Reinforced Polymer Composite for Bullet Proof and Ballistic Applications. *Polymers* **2021**, 13. [CrossRef] [PubMed]
5. de Queiroz, H.F.M.; Banea, M.D.; Cavalcanti, D.K.K. Adhesively bonded joints of jute, glass and hybrid jute/glass fibre-reinforced polymer composites for automotive industry. *Appl. Adhes. Sci.* **2021**, *9*, 2. [CrossRef]
6. Wang, B.; Yan, L.; Kasal, B. A review of coir fibre and coir fibre reinforced cement-based composite materials (2000–2021). *J. Clean. Prod.* **2022**, *338*, 130676. [CrossRef]
7. Neto, J.S.S.; de Queiroz, H.F.M.; Aguiar, R.A.A.; Banea, M.D. A Review on the Thermal Characterisation of Natural and Hybrid Fiber Composites. *Polymers* **2021**, *13*, 4425. [CrossRef]
8. Bourchak, M.; Ajaj, R.; Khalid, M.; Juhany, K.A.; Arun Prakash, V.R.; Alshahrani, H. Development of light weight sustainable pineapple/kevlar hybridized fiber and peanut husk cellulose toughened vinyl ester biocomposite for unmanned aerial vehicle applications. *J. Vinyl Addit. Technol.* **2023**, *29*, 448–457. [CrossRef]
9. Lekrine, A.; Belaadi, A.; Makhlouf, A.; Amroune, S.; Bourchak, M.; Satha, H.; Jawaid, M. Structural, thermal, mechanical and physical properties of Washingtonia filifera Fibres Reinforced Thermoplastic Biocomposites. *Mater. Today Commun.* **2022**, *2022*, 103574. [CrossRef]
10. Belaadi, A.; Boumaaza, M.; Alshahrani, H.; Bourchak, M.; Jawaid, M. Drilling performance prediction of HDPE/Washingtonia fiber biocomposite using RSM, ANN, and GA optimization. *Int. J. Adv. Manuf. Technol.* **2022**, *123*, 1543–1564. [CrossRef]

11. Ku, H.; Wang, H.; Pattarachaiyakoop, N.; Trada, M. A review on the tensile properties of natural fiber reinforced polymer composites. *Compos. Part B Eng.* **2011**, *42*, 856–873. [CrossRef]
12. Jawaid, M.; Alothman, O.Y.; Saba, N.; Tahir, P.M.; Khalil, H.P.S.A. Effect of fibers treatment on dynamic mechanical and thermal properties of epoxy hybrid composites. *Polym. Compos.* **2015**, *36*, 1669–1674. [CrossRef]
13. Glória, G.O.; Teles, M.C.A.; Lopes, F.P.D.; Vieira, C.M.F.; Margem, F.M.; Gomes, M.d.A.; Monteiro, S.N. Tensile strength of polyester composites reinforced with PALF. *J. Mater. Res. Technol.* **2017**, *6*, 401–405. [CrossRef]
14. Rajesh, M.; Pitchaimani, J. Dynamic mechanical and free vibration behavior of natural fiber braided fabric composite: Comparison with conventional and knitted fabric composites. *Polym. Compos.* **2018**, *39*, 2479–2489. [CrossRef]
15. Senthilkumar, K.; Saba, N.; Chandrasekar, M.; Jawaid, M.; Rajini, N.; Siengchin, S.; Ayrilmis, N.; Mohammad, F.; Al-Lohedan, H.A. Compressive, dynamic and thermo-mechanical properties of cellulosic pineapple leaf fibre/polyester composites: Influence of alkali treatment on adhesion. *Int. J. Adhes. Adhes.* **2021**, *106*, 102823. [CrossRef]
16. Müller-Pabel, M.; Rodríguez Agudo, J.A.; Gude, M. Measuring and understanding cure-dependent viscoelastic properties of epoxy resin: A review. *Polym. Test.* **2022**, *114*, 107701. [CrossRef]
17. Saba, N.; Paridah, M.T.; Abdan, K.; Ibrahim, N.A. Dynamic mechanical properties of oil palm nano filler/kenaf/epoxy hybrid nanocomposites. *Constr. Build. Mater.* **2016**, *124*, 133–138. [CrossRef]
18. Asim, M.; Jawaid, M.; Nasir, M.; Saba, N. Effect of Fiber Loadings and Treatment on Dynamic Mechanical, Thermal and Flammability Properties of Pineapple Leaf Fiber and Kenaf Phenolic Composites. *J. Renew. Mater.* **2018**, 6. [CrossRef]
19. Asim, M.; Jawaid, M.; Khan, A.; Asiri, A.M.; Malik, M.A. Effects of Date Palm fibres loading on mechanical, and thermal properties of Date Palm reinforced phenolic composites. *J. Mater. Res. Technol.* **2020**, *9*, 3614–3621. [CrossRef]
20. Asim, M.; Jawaid, M.; Paridah, M.T.; Saba, N.; Nasir, M.; Shahroze, R.M. Dynamic and thermo-mechanical properties of hybridized kenaf/PALF reinforced phenolic composites. *Polym. Compos.* **2019**, *40*, 3814–3822. [CrossRef]
21. Shaikh, H.; Alothman, O.Y.; Alshammari, B.A.; Jawaid, M. Dynamic and thermo-mechanical properties of polypropylene reinforced with date palm nano filler. *J. King Saud Univ. Sci.* **2023**, *35*, 102561. [CrossRef]
22. Jawaid, M.; Awad, S.; Fouad, H.; Asim, M.; Saba, N.; Dhakal, H.N. Improvements in the thermal behaviour of date palm/bamboo fibres reinforced epoxy hybrid composites. *Compos. Struct.* **2021**, *277*, 114644. [CrossRef]
23. Gheith, M.H.; Aziz, M.A.; Ghori, W.; Saba, N.; Asim, M.; Jawaid, M.; Alothman, O.Y. Flexural, thermal and dynamic mechanical properties of date palm fibres reinforced epoxy composites. *J. Mater. Res. Technol.* **2019**, *8*, 853–860. [CrossRef]
24. Sreenivasan, V.S.; Rajini, N.; Alavudeen, A.; Arumugaprabu, V. Dynamic mechanical and thermo-gravimetric analysis of Sansevieria cylindrica/polyester composite: Effect of fiber length, fiber loading and chemical treatment. *Compos. Part B Eng.* **2015**, *69*, 76–86. [CrossRef]
25. Khan, A.; Asiri, A.M.; Jawaid, M.; Saba, N. Inamuddin Effect of cellulose nano fibers and nano clays on the mechanical, morphological, thermal and dynamic mechanical performance of kenaf/epoxy composites. *Carbohydr. Polym.* **2020**, *239*, 116248. [CrossRef]
26. Cebe, P.; Thomas, D.; Merfeld, J.; Partlow, B.P.; Kaplan, D.L.; Alamo, R.G.; Wurm, A.; Zhuravlev, E.; Schick, C. Heat of fusion of polymer crystals by fast scanning calorimetry. *Polymer (Guildf).* **2017**, *126*, 240–247. [CrossRef]
27. Loganathan, S.; Valapa, R.B.; Mishra, R.K.; Pugazhenthi, G.; Thomas, S. Chapter 4—Thermogravimetric Analysis for Characterization of Nanomaterials. In *Micro and Nano Technologies*; Thomas, S., Thomas, R., Zachariah, A.K., Mishra, R., Eds.; Elsevier: Amsterdam, The Netherlands, 2017; pp. 67–108, ISBN 978-0-323-46139-9.
28. Ahmed, M.J.; Balaji, M.S.; Saravanakumar, S.S.; Sanjay, M.R.; Senthamaraikannan, P. Characterization of Areva javanica fiber—A possible replacement for synthetic acrylic fiber in the disc brake pad. *J. Ind. Text.* **2019**, *49*, 294–317. [CrossRef]
29. Mandal, A.; Chakrabarty, D. Studies on the mechanical, thermal, morphological and barrier properties of nanocomposites based on poly(vinyl alcohol) and nanocellulose from sugarcane bagasse. *J. Ind. Eng. Chem.* **2014**, *20*, 462–473. [CrossRef]
30. Kim, H.-S.; Yang, H.-S.; Kim, H.-J.; Park, H.-J. Thermogravimetric analysis of rice husk flour filled thermoplastic polymer composites. *J. Therm. Anal. Calorim.* **2004**, *76*, 395–404. [CrossRef]
31. Gañán, P.; Mondragon, I. Thermal and degradation behavior of fique fiber reinforced thermoplastic matrix composites. *J. Therm. Anal. Calorim.* **2003**, *73*, 783–795. [CrossRef]
32. Choudhury, A. Isothermal crystallization and mechanical behavior of ionomer treated sisal/HDPE composites. *Mater. Sci. Eng. A* **2008**, *491*, 492–500. [CrossRef]
33. Araújo, J.R.; Waldman, W.R.; De Paoli, M.A. Thermal properties of high density polyethylene composites with natural fibres: Coupling agent effect. *Polym. Degrad. Stab.* **2008**, *93*, 1770–1775. [CrossRef]
34. Pistor, V.; Ornaghi, F.G.; Ornaghi, H.L.; Zattera, A.J. Dynamic mechanical characterization of epoxy/epoxycyclohexyl–POSS nanocomposites. *Mater. Sci. Eng. A* **2012**, *532*, 339–345. [CrossRef]
35. García-Martínez, J.M.; Areso, S.; Collar, E.P. Preliminary dynamic-mechanical analysis of polypropylene/short carbon fibers composites modified by a succinic anhydride-grafted atactic polypropylene. *Polym. Eng. Sci.* **2017**, *57*, 731–738. [CrossRef]
36. Asim, M.; Paridah, M.T.; Saba, N.; Jawaid, M.; Alothman, O.Y.; Nasir, M.; Almutairi, Z. Thermal, physical properties and flammability of silane treated kenaf/pineapple leaf fibres phenolic hybrid composites. *Compos. Struct.* **2018**, *202*, 1330–1338. [CrossRef]
37. Idicula, M.; Malhotra, S.K.; Joseph, K.; Thomas, S. Effect of layering pattern on dynamic mechanical properties of randomly oriented short banana/sisal hybrid fiber-reinforced polyester composites. *J. Appl. Polym. Sci.* **2005**, *97*, 2168–2174. [CrossRef]

38. Indira, K.N.; Jyotishkumar, P.; Thomas, S. Thermal stability and degradation of banana fibre/PF composites fabricated by RTM. *Fibers Polym.* **2012**, *13*, 1319–1325. [CrossRef]
39. Hameed, N.; Sreekumar, P.A.; Francis, B.; Yang, W.; Thomas, S. Morphology, dynamic mechanical and thermal studies on poly(styrene-co-acrylonitrile) modified epoxy resin/glass fibre composites. *Compos. Part A Appl. Sci. Manuf.* **2007**, *38*, 2422–2432. [CrossRef]
40. Alothman, O.Y.; Jawaid, M.; Senthilkumar, K.; Chandrasekar, M.; Alshammari, B.A.; Fouad, H.; Hashem, M.; Siengchin, S. Thermal characterization of date palm/epoxy composites with fillers from different parts of the tree. *J. Mater. Res. Technol.* **2020**, *9*, 15537–15546. [CrossRef]
41. Jawaid, M.; Khalil, H.P.S.A. Effect of layering pattern on the dynamic mechanical properties and thermal degradation of oil palm-jute fibers reinforced epoxy hybrid composite. *BioResources* **2011**, *6*, 2309–2322. [CrossRef]
42. Saba, N.; Jawaid, M.; Alothman, O.Y.; Paridah, M.T. A review on dynamic mechanical properties of natural fibre reinforced polymer composites. *Constr. Build. Mater.* **2016**, *106*, 149–159. [CrossRef]
43. Ramakrishnan, S.; Krishnamurthy, K.; Rajeshkumar, G.; Asim, M. Dynamic Mechanical Properties and Free Vibration Characteristics of Surface Modified Jute Fiber/Nano-Clay Reinforced Epoxy Composites. *J. Polym. Environ.* **2021**, *29*, 1076–1088. [CrossRef]
44. Karamipour, S.; Ebadi-Dehaghani, H.; Ashouri, D.; Mousavian, S. Effect of nano-CaCO3 on rheological and dynamic mechanical properties of polypropylene: Experiments and models. *Polym. Test.* **2011**, *30*, 110–117. [CrossRef]
45. Majid, M.; Hassan, E.-D.; Davoud, A.; Saman, M. A study on the effect of nano-ZnO on rheological and dynamic mechanical properties of polypropylene: Experiments and models. *Compos. Part B Eng.* **2011**, *42*, 2038–2046. [CrossRef]
46. Hansen, B.; Borsoi, C.; Dahlem Júnior, M.A.; Catto, A.L. Thermal and thermo-mechanical properties of polypropylene composites using yerba mate residues as reinforcing filler. *Ind. Crops Prod.* **2019**, *140*, 111696. [CrossRef]
47. Sreekumar, P.A.; Saiah, R.; Saiter, J.M.; Leblanc, N.; Joseph, K.; Unnikrishnan, G.; Thomas, S. Effect of chemical treatment on dynamic mechanical properties of sisal fiber-reinforced polyester composites fabricated by resin transfer molding. *Compos. Interfaces* **2008**, *15*, 263–279. [CrossRef]
48. Jayanarayanan, K.; Thomas, S.; Joseph, K. Dynamic Mechanical Analysis of in situ Microfibrillar Composites Based on PP and PET. *Polym. Plast. Technol. Eng.* **2009**, *48*, 455–463. [CrossRef]
49. He, W.; Xing, T.; Liao, G.X.; Lin, W.; Deng, F.; Jian, X.G. Dynamic Mechanical Properties of PPESK/Silica Hybrid Materials. *Polym. Plast. Technol. Eng.* **2009**, *48*, 164–169. [CrossRef]
50. Indira, K.N.; Jyotishkumar, P.; Thomas, S. Viscoelastic behaviour of untreated and chemically treated banana Fiber/PF composites. *Fibers Polym.* **2014**, *15*, 91–100. [CrossRef]
51. Jesuarockiam, N.; Jawaid, M.; Zainudin, E.S.; Thariq Hameed Sultan, M.; Yahaya, R. Enhanced Thermal and Dynamic Mechanical Properties of Synthetic/Natural Hybrid Composites with Graphene Nanoplateletes. *Polymers* **2019**, 11. [CrossRef]
52. Shinoj, S.; Visvanathan, R.; Panigrahi, S.; Varadharaju, N. Dynamic mechanical properties of oil palm fibre (OPF)-linear low density polyethylene (LLDPE) biocomposites and study of fibre–matrix interactions. *Biosyst. Eng.* **2011**, *109*, 99–107. [CrossRef]
53. Almeida Júnior, J.H.S.; Ornaghi Júnior, H.L.; Amico, S.C.; Amado, F.D.R. Study of hybrid intralaminate curaua/glass composites. *Mater. Des.* **2012**, *42*, 111–117. [CrossRef]
54. Shahroze, R.M.; Ishak, M.R.; Salit, M.S.; Leman, Z.; Chandrasekar, M.; Munawar, N.S.Z.; Asim, M. Sugar palm fiber/polyester nanocomposites: Influence of adding nanoclay fillers on thermal, dynamic mechanical, and physical properties. *J. Vinyl Addit. Technol.* **2020**, *26*, 236–243. [CrossRef]
55. Asim, M.; Jawaid, M.; Abdan, K.; Ishak, M.R. The Effect of Silane Treated Fibre Loading on Mechanical Properties of Pineapple Leaf/Kenaf Fibre Filler Phenolic Composites. *J. Polym. Environ.* **2018**, *26*, 1520–1527. [CrossRef]
56. Modesti, M.; Lorenzetti, A.; Bon, D.; Besco, S. Thermal behaviour of compatibilised polypropylene nanocomposite: Effect of processing conditions. *Polym. Degrad. Stab.* **2006**, *91*, 672–680. [CrossRef]
57. Bashir, M.A. Use of Dynamic Mechanical Analysis (DMA) for Characterizing Interfacial Interactions in Filled Polymers. *Solids* **2021**, *2*, 6. [CrossRef]
58. Ren, D.; Zheng, S.; Wu, F.; Yang, W.; Liu, Z.; Yang, M. Formation and evolution of the carbon black network in polyethylene/carbon black composites: Rheology and conductivity properties. *J. Appl. Polym. Sci.* **2014**, *131*, 39953. [CrossRef]
59. Anil, A.; E, T.J.; George, G. Dynamic mechanical properties and ageing studies of coir-sisal yarn reinforced polypropylene commingled composites. *Polym. Polym. Compos.* **2023**, *31*, 09673911221150145. [CrossRef]
60. Kanaginahal, G.M.; Hebbar, S.; Shahapurkar, K.; Alamir, M.A.; Tirth, V.; Alarifi, I.M.; Sillanpaa, M.; Murthy, H.C.A. Leverage of weave pattern and composite thickness on dynamic mechanical analysis, water absorption and flammability response of bamboo fabric/epoxy composites. *Heliyon* **2023**, *9*, e12950. [CrossRef]
61. Chokkalingam, V.; Gurusamy, P.; Kingsly, J.J.; Adinarayanan, A. Mechanical, wear, and dynamic mechanical analysis of Indian rice husk biomass ash Si3N4 and twill weaved aloe vera fiber-epoxy composite. *Biomass Convers. Biorefinery* **2023**. [CrossRef]
62. Naveen, J.; Jawaid, M.; Zainudin, E.S.; Sultan, M.T.H.; Yahaya, R.; Abdul Majid, M.S. Thermal degradation and viscoelastic properties of Kevlar/Cocos nucifera sheath reinforced epoxy hybrid composites. *Compos. Struct.* **2019**, *219*, 194–202. [CrossRef]
63. Asim, M.; Jawaid, M.; Fouad, H.; Alothman, O.Y. Effect of surface modified date palm fibre loading on mechanical, thermal properties of date palm reinforced phenolic composites. *Compos. Struct.* **2021**, *267*, 113913. [CrossRef]

64. Devi, L.U.; Bhagawan, S.S.; Thomas, S. Dynamic mechanical analysis of pineapple leaf/glass hybrid fiber reinforced polyester composites. *Polym. Compos.* **2010**, *31*, 956–965. [CrossRef]
65. Jawaid, M.; Abdul Khalil, H.P.S.; Hassan, A.; Dungani, R.; Hadiyane, A. Effect of jute fibre loading on tensile and dynamic mechanical properties of oil palm epoxy composites. *Compos. Part B Eng.* **2013**, *45*, 619–624. [CrossRef]
66. Pothan, L.A.; Oommen, Z.; Thomas, S. Dynamic mechanical analysis of banana fiber reinforced polyester composites. *Compos. Sci. Technol.* **2003**, *63*, 283–293. [CrossRef]
67. Joseph, P.V.; Mathew, G.; Joseph, K.; Groeninckx, G.; Thomas, S. Dynamic mechanical properties of short sisal fibre reinforced polypropylene composites. *Compos. Part A Appl. Sci. Manuf.* **2003**, *34*, 275–290. [CrossRef]
68. Idicula, M.; Malhotra, S.K.; Joseph, K.; Thomas, S. Dynamic mechanical analysis of randomly oriented intimately mixed short banana/sisal hybrid fibre reinforced polyester composites. *Compos. Sci. Technol.* **2005**, *65*, 1077–1087. [CrossRef]
69. Alshammari, B.A.; Saba, N.; Alotaibi, M.D.; Alotibi, M.F.; Jawaid, M.; Alothman, O.Y. Evaluation of Mechanical, Physical, and Morphological Properties of Epoxy Composites Reinforced with Different Date Palm Fillers. *Materials* **2019**, 12. [CrossRef] [PubMed]
70. Romanzini, D.; Lavoratti, A.; Ornaghi, H.L.; Amico, S.C.; Zattera, A.J. Influence of fiber content on the mechanical and dynamic mechanical properties of glass/ramie polymer composites. *Mater. Des.* **2013**, *47*, 9–15. [CrossRef]
71. Manoharan, S.; Suresha, B.; Ramadoss, G.; Bharath, B. Effect of Short Fiber Reinforcement on Mechanical Properties of Hybrid Phenolic Composites. *J. Mater.* **2014**, *2014*, 478549. [CrossRef]
72. Mandal, S.; Alam, S. Dynamic mechanical analysis and morphological studies of glass/bamboo fiber reinforced unsaturated polyester resin-based hybrid composites. *J. Appl. Polym. Sci.* **2012**, *125*, E382–E387. [CrossRef]
73. Kabir, M.M.; Wang, H.; Lau, K.T.; Cardona, F.; Aravinthan, T. Mechanical properties of chemically-treated hemp fibre reinforced sandwich composites. *Compos. Part B Eng.* **2012**, *43*, 159–169. [CrossRef]
74. Babaee, M.; Jonoobi, M.; Hamzeh, Y.; Ashori, A. Biodegradability and mechanical properties of reinforced starch nanocomposites using cellulose nanofibers. *Carbohydr. Polym.* **2015**, *132*, 1–8. [CrossRef] [PubMed]
75. Dufresne, A.; Castaño, J. Polysaccharide nanomaterial reinforced starch nanocomposites: A review. *Starch Stärke* **2017**, *69*, 1500307. [CrossRef]
76. Sookyung, U.; Nakason, C.; Venneman, N.; Thaijaroend, W. Influence concentration of modifying agent on properties of natural rubber/organoclay nanocomposites. *Polym. Test.* **2016**, *54*, 223–232. [CrossRef]
77. Tajvidi, M.; Falk, R.H.; Hermanson, J.C. Effect of natural fibers on thermal and mechanical properties of natural fiber polypropylene composites studied by dynamic mechanical analysis. *J. Appl. Polym. Sci.* **2006**, *101*, 4341–4349. [CrossRef]
78. Han, Y.H.; Han, S.O.; Cho, D.; Kim, H.-I. Dynamic mechanical properties of natural fiber/polymer biocomposites: The effect of fiber treatment with electron beam. *Macromol. Res.* **2008**, *16*, 253–260. [CrossRef]
79. Romanzini, D.; Ornaghi, H.L.; Amico, S.C.; Zattera, A.J. Influence of fiber hybridization on the dynamic mechanical properties of glass/ramie fiber-reinforced polyester composites. *J. Reinf. Plast. Compos.* **2012**, *31*, 1652–1661. [CrossRef]
80. Venkata Deepthi, P.; Sita Rama Raju, K.; Indra Reddy, M. Dynamic mechanical analysis of banana, pineapple leaf and glass fibre reinforced hybrid polyester composites. *Mater. Today Proc.* **2019**, *18*, 2114–2117. [CrossRef]
81. Ridzuan, M.J.M.; Majid, M.S.A.; Afendi, M.; Mazlee, M.N.; Gibson, A.G. Thermal behaviour and dynamic mechanical analysis of Pennisetum purpureum/glass-reinforced epoxy hybrid composites. *Compos. Struct.* **2016**, *152*, 850–859. [CrossRef]
82. Luo, S.; Cao, J.; McDonald, A.G. Esterification of industrial lignin and its effect on the resulting poly(3-hydroxybutyrate-co-3-hydroxyvalerate) or polypropylene blends. *Ind. Crops Prod.* **2017**, *97*, 281–291. [CrossRef]
83. Xu, X.; Liu, F.; Jiang, L.; Zhu, J.Y.; Haagenson, D.; Wiesenborn, D.P. Cellulose Nanocrystals vs. Cellulose Nanofibrils: A Comparative Study on Their Microstructures and Effects as Polymer Reinforcing Agents. *ACS Appl. Mater. Interfaces* **2013**, *5*, 2999–3009. [CrossRef] [PubMed]
84. Debenedetti, P.G.; Stillinger, F.H. Supercooled liquids and the glass transition. *Nature* **2001**, *410*, 259–267. [CrossRef] [PubMed]
85. Lu, H.; Nutt, S. Restricted Relaxation in Polymer Nanocomposites near the Glass Transition. *Macromolecules* **2003**, *36*, 4010–4016. [CrossRef]
86. Wang, X.; Yu, Z.; McDonald, A.G. Effect of Different Reinforcing Fillers on Properties, Interfacial Compatibility and Weatherability of Wood-plastic Composites. *J. Bionic Eng.* **2019**, *16*, 337–353. [CrossRef]